Available online at www.sciencedirect.com

ScienceDirect

Procedia Engineering 80 (2014) 165 – 182

Procedia Engineering

www.elsevier.com/locate/procedia

3rd International Symposium on Aircraft Airworthiness, ISAA 2013

Dynamic characterization of CFRP composite materials – Toward a pre-normative testing protocol – Application to T700GC/M21 material

Julien Berthe[a,b], Eric Deletombe[b], Mathias Brieu[a], Gérald Portemont[b], Pascal Paulmier[c]

[a]*ECLille, LML, F-59650 Villeneuve D'Ascq, France*
[b]*Onera -The French Aerospace Labı F-59045, Lille, Franceı*
[c]*Onera -The French Aerospace Labı F-92322, Châtillon, France*

Abstract

The lack of normalized protocols to perform dynamic material tests could lead to inconsistent results compared to normalized static tests ones, or between different dynamic test campaigns. Such inconsistencies may be problematic when an accurate identification of strain rate dependent material models is needed, from creep to fast dynamics loadings. For instance, changes in the dynamic specimen in-plane geometry compared to the normalized static ones proved to influence the apparent elastic modulus of CFRP materials. In the present work, a pre-normative study of the dynamic specimen geometry is presented. First, a geometrical criterion is proposed for the [+/-45]s specimens that are commonly used (Rosen tension tests) to study the shear behaviour of composite materials, in order to answer the above mentioned consistency issue between static and dynamic test results. Then, several biases are pointed out which appear when using the (various) normative static test exploitation rules to identify the material properties from dynamic test results, which end up to the proposal of general recommendations to calculate CFRP elastic apparent modulus the same and accurate way for static and dynamic tests, and identify advanced visco-elastic models.

© 2014 Published by Elsevier Ltd. This is an open access article under the CC BY-NC-ND license (http://creativecommons.org/licenses/by-nc-nd/3.0/).

Selection and peer-review under responsibility of Airworthiness Technologies Research Center, Beihang University/NLAA.

Keywords : composite materials; dynamic characterisation; test protocols; CFRP; T700GC/M21

1. INTRODUCTION

The literature review in the field of the dynamic characterization of composite fibers reinforced plastic materials reveals that the lack of normative documents (hence of normalized specimens) to perform dynamic material tests could lead to inconsistent results regarding normalized static tests ones, or between

1877-7058 © 2014 Published by Elsevier Ltd. This is an open access article under the CC BY-NC-ND license (http://creativecommons.org/licenses/by-nc-nd/3.0/).
Selection and peer-review under responsibility of Airworthiness Technologies Research Center, Beihang University/NLAA.
doi:10.1016/j.proeng.2014.09.072

different dynamic test campaigns. Such inconsistencies may sometimes not be problematic, if one just wants to get general trends, but are defeating when the accurate identification of strain rate dependent material models is concerned, from creep to fast dynamic loadings. Previous tests performed by ONERA in the past show that a large part of the trouble, as far as the visco-elastic behaviour of the carbon CFRP materials is concerned, was coming from the change of dynamic specimen in-plane geometry, compared to the normalized static one. In the present work, a pre-normative study of the dynamic specimens geometry is presented, in order to answer the above mentioned consistency issue. Mainly, a geometrical criterion was proposed by Berthe et al. in [1] for the $[+/-45]_s$ specimens that are commonly used (Rosen tests) to study the shear behaviour of composite materials. When this simple geometrical criterion is satisfied, the normalized and dynamic specimens – at the same imposed load rate – lead to the same visco-elastic material data. Beside this geometry issue, several normalized protocols exist that can be used to determine the CFRP composite elastic material properties (Young modulus, Poisson coefficient, etc) from static test results. The lack of normalized dynamic tests (hence normalized exploitation rules) also questions the way to use these dynamic test results. In the present work, general recommendations are proposed to calculate the CFRP elastic modulus the same way for static and dynamic tests, to avoid several biases which appear when one wants to use the static exploitation rules to deal with dynamic test results.

In the first part of the paper, a full-spectrum material characterization campaign is performed on the T700GC/M21 CFRP material from creep to fast-dynamic load rates, at mesoscale (ply) level since mesoscale visco-elastic material models are addressed in the present work. Two ply orientations are usually claimed to be strain rate dependent when thermoset carbon reinforced tape materials are concerned: hence $[+/-45]_s$ and $[90]_4$ specimens were tested to characterize the strain rate dependent shear and transverse behaviour of the material, that is mostly controlled by the resin behaviour. The strain rate range that is covered by the dynamic tension tests is from 10^{-3} s^{-1} up to 10^{+2} s^{-1}. Creep tests are performed to enlarge the range (at 10^{-5} s^{-1} and 10^{-4} s^{-1}). The test results on this broad load rate range (creep to fast-dynamics) are presented and discussed to end up with the definition and validation of consistent specimen geometry and test exploitation rules for static and dynamic analysis. In the second part of the paper, the interest of this experimental work is demonstrated by using the obtained consistent T700GC/M21 creep and dynamic test results to characterize advanced visco-elastic models to be used to study the response of composite structures from creep to impact loads: the T700GC/M21 test results from 10^{-5} s^{-1} to 10^{+2} s^{-1} are successfully used to identify the full-spectrum visco-elastic behaviour model proposed by Berthe et al. [2], which is then proven to be able to reproduce the complex evolution of the material behaviour according to the strain rate.

Nomenclature

$\mathbf{C^0}$	Elastic tensor
E_{11}	Elastic Modulus in fibre direction
E_{22}	Elastic Modulus in transverse direction
G_{12}	Elastic modulus in shear direction
ν_{12}	In plane Poisson coefficient
$\boldsymbol{\sigma}$	Cauchy stress

σ_r	Ultimate failure stress
$\boldsymbol{\varepsilon}$	Total strain
$\boldsymbol{\varepsilon}^{ve}$	Viscous strain
s_d	Standard Deviation
L	Photogrammetric facet size
D	Photogrammetric facet distance
T_β	Polymer transition temperature
$\boldsymbol{\xi_i}$	Elementary viscous mechanism
τ_i	Relaxation time of viscous mechanism
μ_i	Weight of viscous mechanism
$g(\boldsymbol{\sigma})$	Non linear function
γ, n	Parameters of the non linear function
$\mathbf{S^0}$	Elastic compliance
$\mathbf{S^R}$	Viscous compliance tensor
n_c, n_0	Parameters of the Gaussian spectrum
n_c^{stat}, n_0^{stat}	Parameters of the static Gaussian spectrum
n_c^{dyn}, n_0^{dyn}	Parameters of the dynamic Gaussian spectrum

2. EXPERIMENTAL ANALYSIS OF STATIC AND DYNAMIC TENSION TEST PROTOCOLS

2.1. NORMALISED QUASI-STATIC TENSION TESTS

The T700GC/M21 test coupons were cut out (using diamond saw) from composite plates that were manufactured by the Composite Materials and Structures Department of ONERA. The material has been cut and the stacking handmade from unidirectional prepreg tape material of theoretical 0.256 mm ply thickness. The curing cycle was the one recommended by the provider: curing temperature of 180°C (2 hours), under 7 bars, with a mean 2.7°C/min temperature growth rate, and a progressive temperature and pressure decrease to end up the process. The coupons surface was prepared and glass/epoxy tabs properly added (glued) to prevent from getting rupture of the specimens in the grips.

Normalized tensile tests have first been performed in order to characterize the quasi-static behaviour of the T700GC/M21 material. Three laminates have been tested $[0]_8$, $[90]_8$ et $[(\pm 45)_2]_s$ in order to identify the different modulus of the in-plane 2D compliance matrix. Several norms [3-5] coexist for such quasi-static tests, which define not only the different specimen geometry (see Table 1.) but also a number of test specimens (namely 5) to be tested to get the standard deviation, the kind of instrumentation to be used to measure the stresses and strains, and the calculation rules to calculate the material mechanical properties (elastic Young modulus, Poisson coefficients) from the stress-strain tests results. These calculation rules differ according to the different norms. Hereafter, the norms that are recommended by Airbus to

characterize composites elastic properties were used, and the values of the elastic parameters obtained from the dynamic tests are compared to those obtained from the quasi-static ones using the ISO formulae. In the present work a maximum of three specimens by test configuration was used because of cost reasons. For the $[0]_8$ laminate, no dynamic test has been performed since the behaviour of CFRP materials in the carbon fibre direction is usually claimed not to be dependent on the loading speed. Quasi-static tests have been made at a measured constant 0.5 mm/min speed on a conventional Instron 5887 testing machine equipped with a 300 kN Kistler piezo-electric load cell. The strains were measured using TML YFLA-2 extensometric strain gauges that were glued both sides of the composite specimens. The quasi-static test results on the $[0]_8$ laminate are presented in Fig. 1(a), with a slightly increasing modulus being observed that could be explained by a fibre re-alignment mechanism due to the presence of thermoplastic nodules in the resin. Once exploited using the NF EN 2561:1996 norm the 3 tests gave the following values for the elastic material parameters in the fibre direction: E_{11} = 136 GPa ±1.3%, ν_{12} = 0.31 ±3.2%.

Table 1. Normalized specimen geometry for tensile tests in composite fibre, transverse and shear directions

Specimen	Length	Width	Thickness	Tabs length	Tabs thickness
$[0]_8$	250 mm	10 mm	2.16 mm	50 mm	1 mm
$[90]_8$	250 mm	25 mm	2.16 mm	50 mm	1 mm
$[(\pm 45°)_2]_S$	230 mm	25 mm	2.16 mm	50 mm	1 mm

A first set of tests in the transverse direction was performed on a $[90]_8$ laminate, using the NF EN 2597:1998 norm [3], which exhibited premature rupture because of the specificity of the Instron 5887 jaws. A second test campaign was then performed on an Instron 4302 testing machine equipped with another gripping system, and a Kistler 10 kN piezo-electric load cell. The different gripping system led the authors to use composite specimens of the same geometry but without tabs. Those tests turned to effectively develop a proper rupture in the free length of the specimens (away from the grips). The strains were measured using TML YFLA-2 extensometric gauges glued both sides of the composite specimens. Three tests were performed to get a first grip on the results standard deviation. The mean ultimate stress was about 75.4 MPa ±6%. A quasi-linear response until rupture can be observed on Fig. 1. With the NF EN 2597:1998 norm, the elastic modulus is calculated as being the secant modulus between points corresponding to $\sigma_r/10$ and $\sigma_r/2$: this rule led to a mean E_{22} value about 8086 MPa ±4.4%.

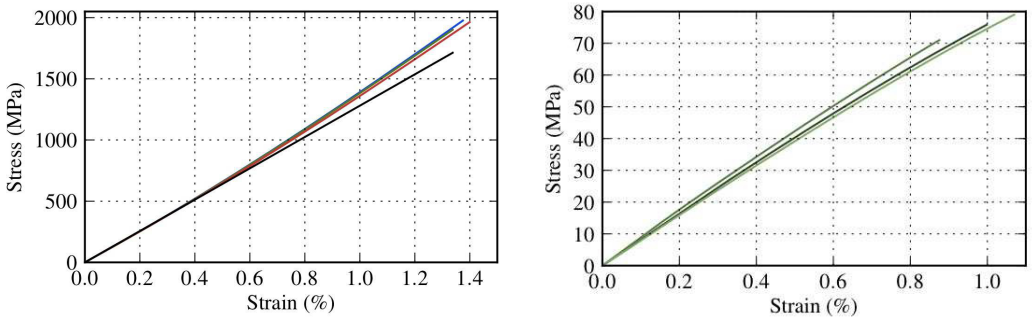

Fig. 1. Stress-strain curves for 3 quasi-static tensile tests by case with normalized specimen geometry for T700GC/M21 (a) fibre direction $[0]_8$; (b) transverse direction $[90]_8$

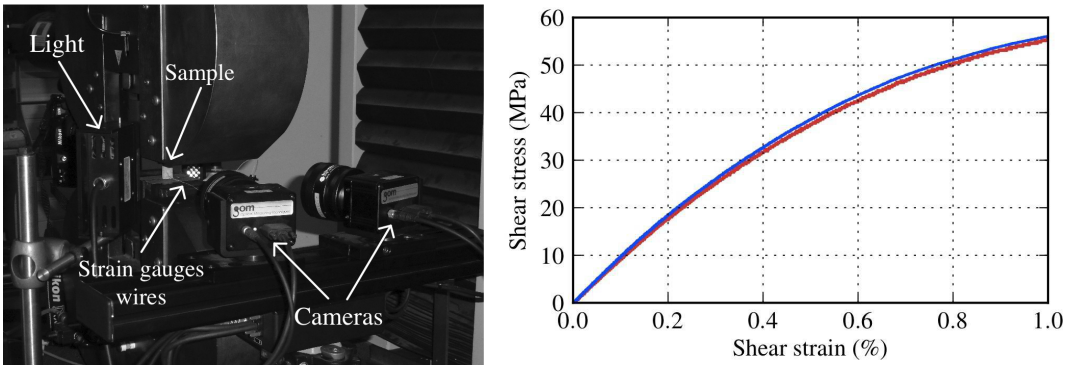

Fig. 2. Quasi-static tensile tests on $[(\pm 45°)_2]_s$ T700GC/M21 specimens (a) experimental test rig; (b) shear stress-strain curves

The ISO 527-5:1997 norm [4] can also be used to identify the E_{22} transverse modulus, with the calculation rule being the same as for the E_{11} fibre direction, (secant modulus between points corresponding to $\varepsilon = 0.05\%$ and $\varepsilon = 0.25\%$). This second rule (using the same test results) gave a mean E_{22} value about 8318 MPa ±5.4%, which is 3% higher than the previous value. This can be easily explained because the load level that is used in the NF EN 2597:1998 norm is higher than in the ISO 527-5:1997 norm and the T700GC/M21 material behaviour is slightly non-linear with a decreasing tangent modulus in the transverse direction.

Quasi-static tensile tests on a $[(\pm 45)_2]_s$ laminate were then performed to characterize the shear behaviour of T700GC/M21, using the AITM 1-0002:1998 norm [5]. The Instron 5887 conventional testing machine was used, with the quasi-static tests being done at a constant 0.5 mm/min test speed. The same piezo-electric cell and extensometric strain gauges were used to get the stress-strain curves (see Fig. 2., where the test results are shown up to 1% strain to better focus on the elastic response (the ultimate non-linear strain is over 6%). Only two tests were performed because of limitation in the available number of specimens. The shear modulus is calculated both in the AITM 1-0002:1998 and the NF EN ISO 14129:1998 norms as being the secant modulus between points that correspond to $\varepsilon = 0.05\%$ et $\varepsilon = 0.25\%$: the mean G_{12} shear modulus was about 4351 MPa ±3%.

2.2. Improvement of the tensile test specimen geometry for dynamic tests

As it will be seen, some of the T700GC/M21 previously studied material properties depend on the test speed. But no normalized specimen definition or calculation rules exist to measure the elastic material properties of composite materials under dynamic loadings. Since the existing tensile hydraulic testing machines cannot reach as high test speeds and loads as one could desire, several solutions are usually proposed to cover a larger range of strain rates: the first one consists in using thinner (for load capacity) and shorter (for strain rate capacity) specimens; the second consists in using very specific testing machines such as Split Hopkinson Bars. In both case the specimens scale and geometry change - compared to what the previously mentioned norms recommend for quasi-static tests - in such an extent that an influence on the test results and calculated material parameters can be observed. Then the question of the consistency of results and material parameters that are calculated from different test protocols raises. Hence various types of different tests have been performed on conventional testing machines to validate test protocols that could contribute to the accurate and consistent characterization of the strain

rate dependence of the T700GC/M21 composite material behaviour from quasi-static (10^{-5} s^{-1}) to medium test speeds (10^{+2} s^{-1}). For that purpose, the ONERA dynamic specimen geometry (see Table 2.) was evaluated and compared to normalized quasi-static geometry, by using both controlled constant (low) strain rates and imposed (high) tensile speeds testing machines and protocols. In order to limit the dynamic excitation of the piezo-electric cell during the dynamic tests that spoils the exploitation process, ONERA usually use dynamic specimens which are thinner than the normalized ones (4 plies instead of 8): the influence of the specimen thickness on the test results and calculated elastic material parameters is indeed negligible compared to geometry effects (as shown later). These tests have only been performed on [±45°] and [90°] laminates since no dynamic dependence was expected for the [0°] laminate.

Table 2. Initial specimen geometry for dynamic characterization of T700GC/M21

Specimen	Length	Width	Thickness	Tabs length	Tabs thickness
$[90]_8$ Static	250 mm	25 mm	2.16 mm	50 mm	1 mm
$[90]_4$ Dynamic	130 mm	20 mm	1.08 mm	50 mm	1 mm
$[(\pm 45°)_2]_S$ Static	230 mm	10 mm	2.16 mm	50 mm	1 mm
$[\pm 45°]_S$ Dynamic	130 mm	25 mm	1.08 mm	50 mm	1 mm

A photogrammetric measurement of the tensile strain field of the specimen was proposed by Berthe et al. [1] to equip the tensile imposed speed tests: for that purpose a black & white random pattern was painted on the specimen surfaces, and two synchronised BASLER high resolution (1620x1024) 24 fr/s video cameras were used to record the B&W pattern displacements. Schneider-Kreuznach 50-mm f/2.8 optical systems were used in order to get full pictures of a 35 mm x 28 mm zone of interest which was large enough to almost completely cover the surface of the dynamic specimens. In that configuration, each pixel covered a 21µm x 21µm area. For the normalized specimens, the 35 mm x 28 mm pictures were centred where the extensometric strain gauges are usually glued (centre of the specimens). Hence a stereo-digital image correlation analysis could be performed using the Aramis 6.1 software (GOM company) to measure the in-plane and out-of plane displacements then deformation of the studied specimens accurately. To compute displacements, the pictures are split into small facets of several pixels size (L), each facet centre being distant from its neighbours by a distance D that is lesser or equal to L. For the present study, the different values for L and D were: L = 24 pixels, D = 12 pixels.

The test campaign performed on the Instron 4302 testing machine with ONERA $[90]_4$ dynamic specimens compared to the $[90]_8$ normalized ones gave the following results: the imposed speed of the loading beam was 10 mm/min for the normalized specimens and 5 mm/min for the dynamic ones, which gave strain rates in the linear strain domain of the same order of magnitude: 6.10^{-4} s^{-1} and 12.10^{-4} s^{-1} respectively. Strain maps are presented in Fig. 3. for an average strain level which corresponds to the upper value used in the norm to calculate the elastic modulus (ε =0.49% for the normalized geometry ε =0.48% for the dynamic one). The observed strain fields are homogeneous and similar for both geometries, with a standard deviation about 0.049% only. In the $[90°]_4$ case the specimen geometry does not need to be improved. This result has been confirmed when testing both specimen geometries using a quasi-static 5.10^{-4} s^{-1} controlled strain rate protocol on an electro-mechanical Instron 5800R testing machine. The longitudinal strain was measured with an extensometer which was stick on one side of the specimens in order to accurately measure and control the strain rate during test. The mechanical strain was obtained using longitudinal strain gauges.

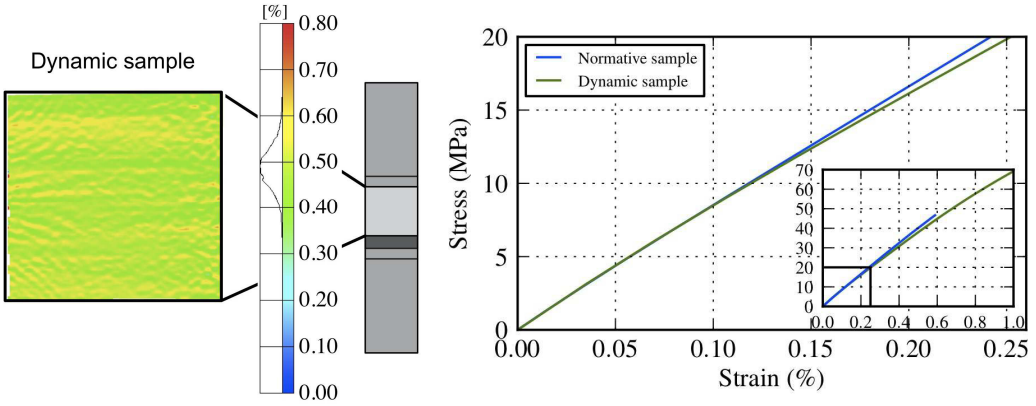

Fig. 3. Tensile tests at imposed velocity (left) or controlled strain rate (right) on $[90]_8$ T700GC/M21 laminate (a) strain field distribution for the dynamic specimen geometry; (b) comparison of stress/strain curves for the normalized and dynamic specimens.

The test results are shown in Fig. 3. Clearly the Young modulus are very close to each other up to ε =0.125%. The increasing difference after this strain level can easily be explained because of the different evolution of damage in the specimens because of their different thickness. The ultimate strain and strain are very different: specimens with tabs have been used, and rupture occurred between these tabs. As previously discussed, the use of the NF EN 2597:1998 norm to calculate the Young modulus does not seem to be relevant because of these very different ultimate stresses. Considering and adapting the ISO 527-5:1997 norm, the Young modulus was calculated between pre-determined ε =0.05% and ε =0.15% strain levels and the calculated E_{22} modulus was then about 8090 MPa for the normalized specimen and 7870 MPa for the dynamic one. A 2.7% difference only was then observed between the different geometries.

Concerning the imposed velocity test results and the photogrammetric measurements (strain fields) done on the [±45°] laminate, the tests have been performed using the electro-mechanical Instron 5887 testing machine. The same parameters as previously mentioned have been used for the stereo digital correlation measurements (pixel and facet sizes). In order to get strain rates of the same order of magnitude, an imposed 10 mm/min test speed has been used for the normalized specimens and a 5 mm/min test speed for the dynamic specimens, which gave respectively a 4.10^{-4} s^{-1} and 8.10^{-4} s^{-1} approximate strain rate in the linear strain range. In Fig. 4. the average strain level for the normalized and dynamic geometries is respectively about ε =0.31% and ε =0.36%, which corresponds to the upper strain value that is used in the AITM 1-0002:1998 norm to calculate the elastic modulus. The strain distribution was clearly more homogeneous for the normalized specimen compared to the dynamic one, with a standard deviation s_d about 0.043% and 0.152% respectively. This difference can partly be explained because of the proximity of the strain gauge with the load introduction in the tabs in the case of the dynamic geometry. Plus the strain was not homogeneous along the section of the dynamic specimen (see Fig. 4.). This was clearly pointed out when the load increased and three areas appeared with very different strain levels: when in the first one close to the tabs the longitudinal strain level was lower (ε =1.25%), in the second area at mid-section of the specimen but close to the edges the strain level was higher (ε =2.24%), and in the last central area of the specimen the strain level was maximum (ε =3.09%). The average strain level at the mid-section of the specimen was clearly different from the one measured by the strain gauge that was set at the centre of the specimen : the calculated Young modulus cannot be obtained

properly using this dynamic geometry, compared to the normalized geometry which gives an homogeneous strain along the mid-section of the specimens. To avoid such a localisation effect with the short dynamic geometry, Berthe et al. proposed to decrease the width of the specimens to be less than half its length [1].

The stereo digital correlation results are presented in Fig. 4. for both the initial and improved dynamic geometries. The dimensions of the specimens are given in Table 3. The standard deviation of strain along the mid-section of the improved geometry was largely reduced down to 0,039% and a much more homogeneous strain was obtained along this section.

Table 3. Improved dynamic specimen geometry for the [±45°]s shear tests

Specimen	Length	Width	Thickness	Tabs length	Tabs thickness
$[\pm 45°]_S$ Dynamic	130 mm	25 mm	1.08 mm	50 mm	1 mm
[±45°]s Improved	130 mm	15mm	1.08 mm	50 mm	1 mm

In order to definitely validate the improved dynamic geometry, controlled 5.10^{-4} s^{-1} strain rate tests were performed using the same protocol as the one previously described. The stress/strain curves are plotted in Fig. 5. The normalized quasi-static and improved dynamic geometries exhibited almost the same elastic modulus up to a 0.125% strain level. The elastic modulus is calculated for the three geometries using the AITM 1-0002:1998 norm (calculated between ε =0.05% and ε =0.25%). The shear modulus was about 4330 MPa, 3440 MPa (-20.6%) and 4110 MPa (-5.1%) respectively for the normalized, initial dynamic and improved dynamic geometry. Differences between the specimens increase together with the load level (above 0.15%), which is due to different initiation and evolution of damage according to the specimens thickness and dimensions. It is important to remind here that the $[\pm 45°]_s$ specimens were proposed by Rosen [6] to measure the shear modulus of fibre reinforced composite materials, who already warned his readers that great care should be taken when using his proposed protocol to characterize non linear anelastic behaviour of composite materials.

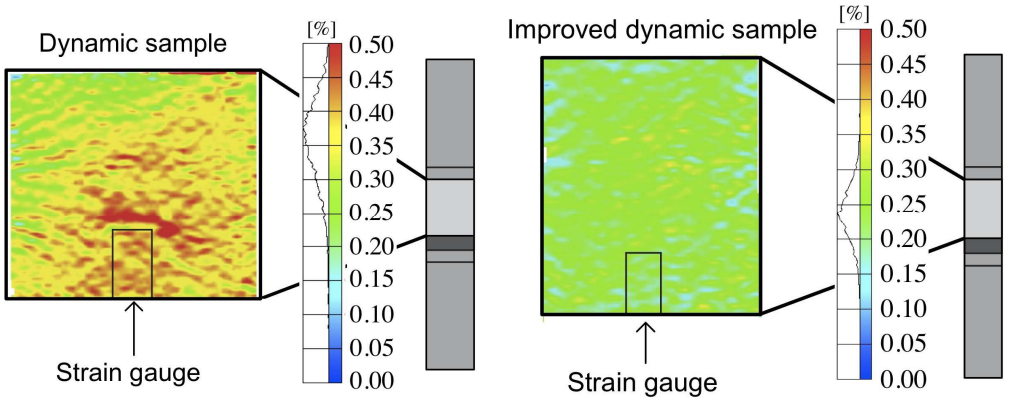

Fig. 4. Comparison of the longitudinal strain field for an average 0.25% strain level and T700GC/M21 $[\pm 45°]_s$ laminate (a) initial dynamic geometry; (b) improved dynamic geometry

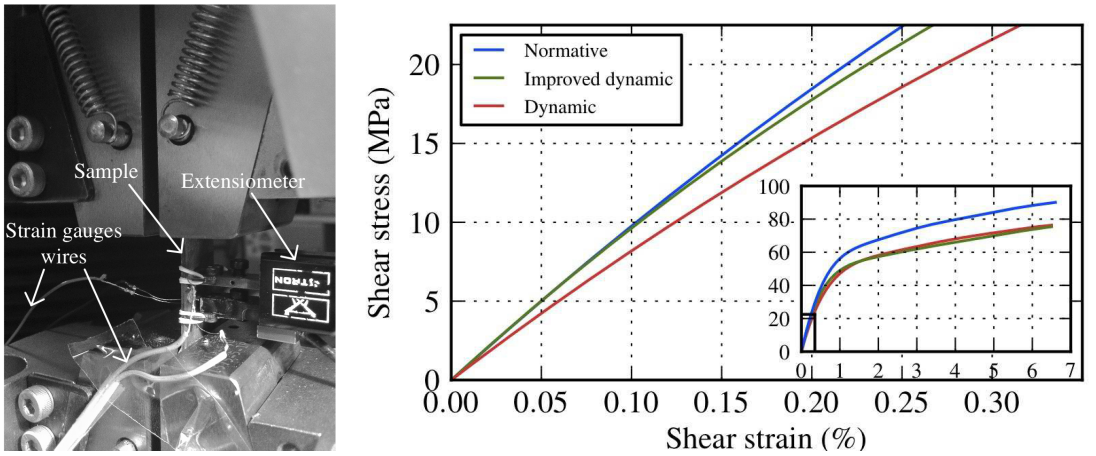

Fig. 5. Longitudinal tensile tests at imposed test speed for T700GC/M21 [±45°] laminates (a) experimental test rig; (b) stress/strain curves

2.3. Mechanical chracterisation of T700GC/M21 material on a large loading speed range

A dynamic test campaign was performed using the ONERA Schenck hydraulic jack and the studied dynamic specimen geometry. The description of the test rig is given in Fig. 6. The test speed corresponds to the imposed speed of the vertical loading bar. The lower grip is clamped to the cast-iron plate, with a ±200 kN piezo-electric force cell (Kistler 9071A) being set between these two parts to measure the mechanical load. The upper grip displacement is measured by a LC 2450 Keyence laser system. The longitudinal and transverse strains are obtained thanks to extensometric (TML YFLA-2) strain gauges. A 1 MHz data acquisition system is used to record the dynamic data, which are analysed using the FAMOS IMC software.

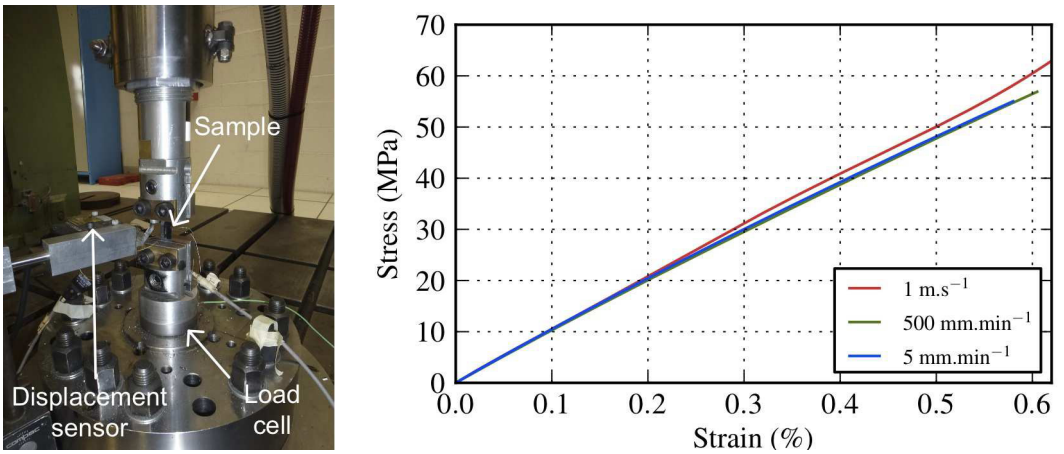

Fig. 6. Longitudinal dynamic tensile test on a $[90]_4$ T700GC/M21 laminate (a) experimental test rig; (b) mean stress/strain curves for different test speeds

The FAMOS IMC software is needed for various reasons: First the force signal must be accurately synchronised with the strain signal (the transient force and strain signals are not measured at the same location) to get a proper dynamic stress/strain curve hence initial elastic modulus. Second, under dynamic loadings a very high frequency and possibly high amplitude content is delivered by the piezo-electric cell due to its high stiffness and eigen-frequencies. These eigen-frequencies are well known (using a Fast Fourier Transform of the raw force signal reveals a parasitic content in the 5-8 kHz bandwidth), and can easily be filtered (a Butterworth filter is traditionally used). This filtering operation is only required for impact speeds over 500 mm/min.

Dynamic tensile tests at various test speeds were performed in the transverse direction on $[90]_4$ T700GC/M21 dynamic specimens. For each test speed three tests were done in order to check repeatability. Some of the stress/strain curves are plotted in Fig. 6. where a very small difference appears up to a 0.2% strain level whatever the test speed (the 1 m/s, 500 mm/min and 5 mm/min correspond respectively to strain rates about 21 s^{-1}, 0.11 s^{-1} et 1.10^{-3} s^{-1}). The T700GC/M21 transverse behaviour was then claimed to be hardly visco-elastic.

The improved dynamic specimen geometry was then used to characterize the T700GC/M21 shear elastic behaviour (Rosen tests). Tensile tests at various test speeds were performed, with three tests being done for each test speed to check dispersion. Some of the obtained stress/strain curves are plotted in Fig. 7 (a). and an important evolution of the shear behaviour according to the test speed can be pointed out (the 2 m/s, 1 m/s, 0.5 m/s, 500 mm/min, 50 mm/min and 5 mm/min test speeds correspond respectively to strain rates about 50 s^{-1}, 25 s^{-1}, 16 s^{-1}, 0.1 s^{-1}, 7.10^{-3} s^{-1} and 1.10^{-3} s^{-1}). Intermediate 1 s^{-1} strain rate tests were performed but discarded because of a mechanical perturbation due to the test rig (discontinuous contact between sliding block and loading beam at this specific test speed).

The use of the AITM 1-0002:1998 norm that was used to calculate the quasi-static shear elastic modulus with the normalized specimen geometry (between ε =0.05% and ε =0.25%) gave the results in Table 4 and Fig. 7 (b) once applied to the dynamic test data. An important elastic shear modulus increase was observed from 10^{-3} s^{-1} to 50 s^{-1} (45%).

Table 4. Apparent transverse and shear modulus of the $[90]_8$ and $[\pm45°]_S$ T700GC/M21 specimens according to the strain rate, calculated with the AITM-0002-1998 norm

	1.10^{-3} s^{-1}	0.11 s^{-1}	21 s^{-1}
E_{22} (MPa)	10214	10106	10557
Deviation	3%	3.4%	3.5%

	1.10^{-3} s^{-1}	7.10^{-3} s^{-1}	0.1 s^{-1}	16 s^{-1}	25 s^{-1}	50 s^{-1}
G_{12} (MPa)	4565	4786	5089	5634	6073	6621
Deviation	2.1%	1.2%	3.9%	5.6%	3.8%	3.8%

The evolution of elastic shear modulus was moderate until 10 s^{-1} then became much larger. These results prove the interest in characterising the strain rate sensitivity finely, where it is usually coarsely done in the literature for only 3 strain rates of very different ranges (quasi-static and medium strain rates with hydraulic machines and high strain rates with Split Hopkinson Bars).

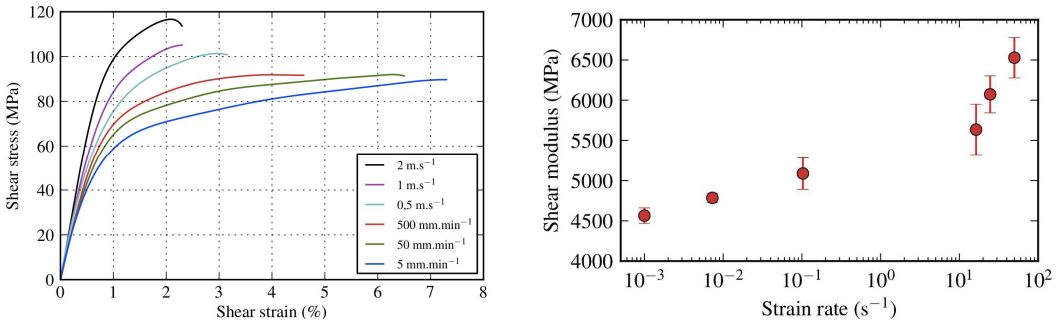

Fig. 7. Tensile dynamic tests on a $[\pm 45°]_S$ T700GC/M21 laminate (a) stress/strain curves; (b) apparent shear modulus according to the strain rate

The slope change in the strain rate dependency of the shear elastic modulus has been further confirmed and justified by Berthe [7], as being due to the shift of the T_β characteristic transition temperature of the M21 resin with the strain rate (time-temperature equivalence in polymers) from about -80 °C (at 10^{-3} s^{-1}) to +20 °C (at 10 s^{-1}).

During these dynamic tests, the stress interval between ε =0.05% and ε =0.25% (AITM 1-0002:1998 norm) increases from [9.2 MPa; 46 MPa] to [14 MPa; 70 MPa] respectively for the 5 mm/min and 2 m/s test results. With the change in the upper stress value, the damage amount on the stress interval used to calculate the shear modulus could turn to be quite different, meaning that the elastic modulus is calculated for an undamaged specimen at lowest test speed and possibly a damaged one at highest speed. Indeed, Huchette [8] previously recorded noticeable acoustic events during tensile longitudinal tests performed on a [±45°] T700/M21 laminate after 60 MPa. If the elastic modulus is calculated on a [9.2 MPa; 46 MPa] stress interval, the obtained value for the 2 m/s dynamic test is 2% higher than when calculated on the [14 MPa; 70 MPa] interval, and the standard deviation s_d of the calculated shear modulus for the three 2 m/s tests is reduced by 20%. The elastic shear modulus given in Table 5 is obtained using this rule. The dynamic dependency is slightly increased, and the s_d notably reduced. The main conclusion here is that new rules should perhaps be defined by the norms to characterize the elastic behaviour of CFRP composite laminates when considering possible strain rate sensitivity.

Table 5. Apparent elastic shear modulus of T700GC/M21 material calculated on the [9.2 MPa; 46 MPa] stress interval for different strain rates

	1.10^{-3} s^{-1}	7.10^{-3} s^{-1}	0.1 s^{-1}	16 s^{-1}	25 s^{-1}	50 s^{-1}
G_{12} (MPa)	4565	4822	5181	5706	6195	6660
Deviation	2.1%	2.2%	2.9%	3.6%	3.0%	2.7%

3. IDENTIFICATION OF BERTHE'S VISCOELASTIC SPECTRAL MODEL ON A BROAD RANGE OF STRAIN RATES

3.1. CREEP TEST RESULTS ON T700GC/M21

In order to characterize the T700GC/M21 behaviour for very low strain rates, creep tests have been performed by the ONERA Composite Materials and Structures Department. These tests have been done

using an electro-mechanical ZWICK testing machine equipped with a 150 kN load cell, with the previously described improved specimen geometry (which was used for the dynamic tests). The longitudinal and transverse strains were measured using VISHAY CEA-06-125WT-350 strain gauges. Both the $[\pm 45°]_S$ and the $[90°]_4$ laminates have been studied. The creep tests consisted in several 1000s loading steps (see Fig. 8.) in order to characterize the non linear creep behaviour of the T700GC/M21 material.

For the $[90°]_4$ tests, three load levels of 15 MPa, 31 (15+16) MPa et 47 (31+16) MPa have been selected. On the stress/strain curves plotted in Fig. 8. a small non linear visco-elastic response is observed. The corresponding strain rate during the constant stress load steps has been estimated for each step between t=250 s and t=950 s, then a 2.74 10^{-6} s^{-1} strain rate is obtained for the first (15 MPa) load step, a 3.8 10^{-6} s^{-1} for the second (31 MPa) load step, and 123. 10^{-5} s^{-1} for the last one (47 MPa). Few and low energy acoustic events were recorded during the first loading step and before 20 MPa. Their number and cumulated energy increase notably after 25 MPa. The material response after the first load plateau should then not be used to characterize the purely visco-elastic behaviour in the transverse direction of the material.

For the $[\pm 45°]_s$ specimens, four load steps were selected for the creep tests : 31 MPa, 62 (31+31) MPa, 95 (62+33) MPa and 127 (95+32) MPa. The observed results on Fig. 8 reveal a highly non linear visco-elastic shear behaviour of the T700GC/M21 material. The viscous strain evolution can be calculated during each load step (final strain minus initial strain at the onset of the load step) which gives 0.030%, 0.074%, 0.234% and 1.51% viscous strains respectively for the 31 MPa, 62 MPa, 95 MPa and 127 MPa load steps. The viscous strain rates are 1. 10^{-5} s^{-1}, 2. 10^{-5} s^{-1}, 1. 10^{-4} s^{-1} and 7. 10^{-4} s^{-1} for the 31 MPa, 62 MPa, 95 MPa and 127 MPa load steps. As in Schieffer [9] a clearly non linear evolution of the viscous strain rate is observed. Few and low energy acoustic events appeared during the second load step (over 60 MPa): some damage at the microscopic scale probably develop (fiber/matrix debonding) which has little effect on the macroscopic behaviour of the laminate as reported by Lecomte et al. [10]. Then the acoustic activity really increased after 120 MPa. These results are in agreement with those obtained by Huchette with another specimen geometry. For these shear tests, it was then assumed that few damage developed during the first three load steps: the purely elastic shear modulus can then still be characterized using these first load steps.

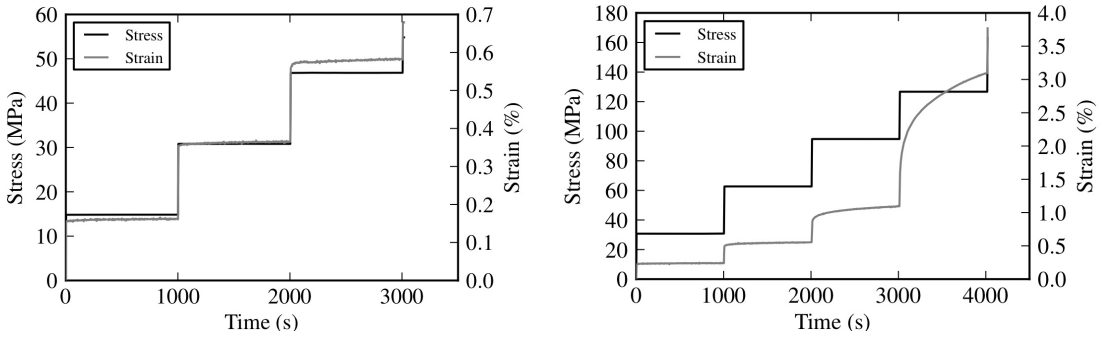

Fig. 8. Multiple step creep tests results on the T700GC/M21 composite material (a) in transverse direction $[90]_4$; (b) in shear direction $[(\pm 45°)_2]_S$

3.2. IDENTIFICATION OF BERTHE'S BI-SPECTRAL VISCO-ELASTIC MODEL FOR THE T700GC/M21 MATERIAL

In the following work a visco-elastic model is studied, which was based on a spectral based creep one proposed by Maire [11] and used by Laurin et al. [12] et Carrère et al. [13] where the visco-elastic behaviour of the ply, in the local basis, can be written as:

$$\sigma = C^0 : (\varepsilon - \varepsilon^{ve}) \tag{1}$$

where $\boldsymbol{\sigma}$ is the Cauchy stress, $\mathbf{C_0}$ the elastic tensor, $\boldsymbol{\varepsilon}$ the total strain and $\boldsymbol{\varepsilon}^{\mathbf{ve}}$ the viscous strain. In such an approach, the viscous strain is taken as the sum of elementary viscous mechanisms $\boldsymbol{\xi_i}$, associated with a relaxation time τ_i and a weight μ_i:

$$\frac{d\varepsilon^{ve}}{dt} = g(\sigma)\sum_i \frac{d\xi_i}{dt} \quad \text{and} \quad \frac{d\xi_i}{dt} = \frac{1}{\tau_i}(\mu_i g(\sigma) S^R : \sigma) - \xi_i \tag{2}$$

with g($\boldsymbol{\sigma}$) a non-linear function and $\mathbf{S^R}$ the viscous compliance, which are defined hereafter. This model can be seen as a generalization of rheologic models with an important number of springs and dashpots. The weight and relaxation times of each elementary viscous mechanism (μ_i and τ_i) define the temporal spectrum. These relaxation times are the classical ones from rheologic models. To be representative, the model needs a large number of viscous mechanisms to be considered (in the rest of this paper 200 mechanisms are arbitrarily used). In order to simplify identification of the temporal spectrum, a Gaussian spectrum form (3) is used.

$$\tau_i = \exp(i) \quad \text{and} \quad \mu_i = \frac{\overline{\mu}_i}{\sum_i \overline{\mu}_i}, \quad \text{with} \quad \overline{\mu}_i = \frac{1}{n_0\sqrt{\pi}} \exp\left(\left(-\frac{i-n_c}{n_0}\right)^2\right) \tag{3}$$

The spectrum is based on only two parameters: n_c the mean of the Gaussian spectrum and $n_0 = \sqrt{2}s_d$ with s_d the standard deviation. The described spectrum has been successfully used by Maire et al. [14] to model the visco-elastic behaviour of glass fibre reinforced polymer (GFRP) during creep test. In order also to simplify identification, the viscous compliance is taken as a function of the elastic compliance $\mathbf{S^0}$. In this model, only viscosity in transverse and shear directions is considered ($\beta_{11} = 0$):

$$\mathbf{S^R} = \begin{pmatrix} 0 & 0 & 0 \\ 0 & \beta_{22} S^0_{22} & 0 \\ 0 & 0 & \beta_{66} S^0_{66} \end{pmatrix} \tag{4}$$

Finally, to describe creep tests, the following nonlinear function g($\boldsymbol{\sigma}$) is introduced:

$$g(\sigma) = 1 + \gamma\left(\sqrt{{}^t\sigma : S^R : \sigma}\right)^n \tag{5}$$

This visco-elastic model is reported to need only two tests to identify its viscous parameters (n_c, n_0, β_{22}, β_{66}, γ and n): a multiple step creep test on a [±45°] laminate and a single creep test on a [90°] laminate, as presented in the previous paragraph.

The model proposed by Berthe et al. [1] is an extension of this model to cover a larger range of dynamic rates, by using a multi-Gaussian spectrum (Fig. 9.). Because of the existence of specific characteristic transition temperatures and considering the general time-temperature equivalence principle in polymers, Berthe found out [7] that a simple Gaussian spectrum could not predict the material stiffness evolution when this temperature (or loading rate) threshold is being crossed. Berthe also demonstrated from the tests (see Fig.7.) that only one transition temperature (T_β) was concerned for the considered [10^{-5} s^{-1}; 10^{+2} s^{-1}] and [-100°C; +100°C] strain rate and temperature ranges. Hence he proposed to superimpose a dynamic Gaussian spectrum (n_c^{dyna} and n_0^{dyna}) with the static Gaussian spectrum (n_c^{stat} and n_0^{stat}), all the other viscous parameters being unique. Equation (3) only has to be re-written in order to take account of this extension, to give equation (6):

$$\mu_i = \frac{\overline{\mu}_i^{dyna}}{\sum_i \overline{\mu}_i^{dyna}} + \frac{\overline{\mu}_i^{stat}}{\sum_i \overline{\mu}_i^{stat}}, \quad \text{with} \quad \overline{\mu}_i^k = \frac{1}{n_0^k \sqrt{\pi}} \exp\left(\left(-\frac{i - n_c^k}{n_0^k} \right)^2 \right) \tag{6}$$

The following identifications have been done using the MATLAB optimisation library, and more specifically the non linear least square fit routine “lsqcurvefit”. In order to avoid well known difficulties regarding possibly existing local minima of the solution function, the solution space has been constrained (after some sensitivity studies had been made) to remain in expectedly physical intervals around existing values found in the literature [11-14]. Several optimisation runs with different initial research points were also performed to prove convergence towards a unique set of parameters.

The model identification was first done for the shear behaviour, regardless of the transverse test results. Since the proposed bi-spectral model only aims at describing the visco-elastic behaviour without damage of the material, only the first part (with a shear stress less than 80 MPa) of the experimental curves where no macroscopic damage is assumed to have developed was used to optimise the material model parameters: five test speeds (creep and dynamic) were used to identify this model.

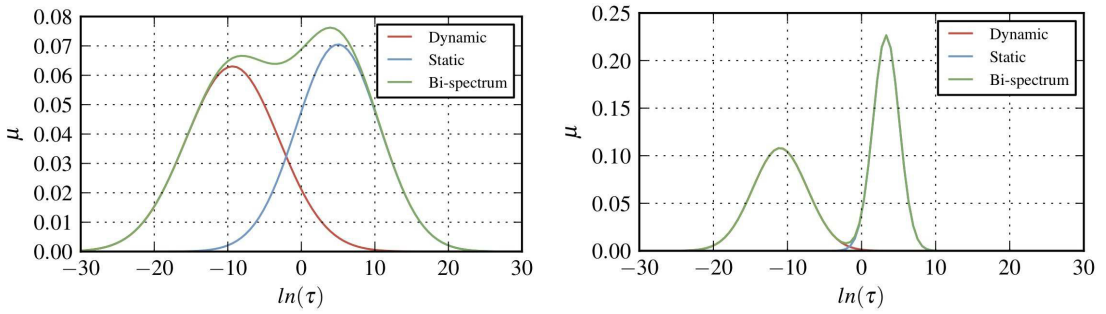

Fig. 9. Berthe’s bi-spectral visco-elastic model (a) concept illustration; (b) identification for the T700GC/M21 material

The obtained parameters values are presented in Table 7. Two astonishingly well dissociated static and dynamic spectrums appeared (see Fig. 9. (b)) which could mean that two different (sets of) viscous mechanisms were activated by the different tests. The comparison between the model and tests stress/strain curves is given in Fig. 10 (a) and Fig. 11 (a) for the dynamic and creep cases respectively. A good correlation is obtained, the mean error (over all the points of the curves) for all test speeds (creep, 5 mm/min, 50 mm/min, 500 mm/min, 1 m/s et 2 m/s) being only 2.65%, with a 0.39% minimum mean error for the 5 mm/min test speed, and a 6.97% maximum mean error for the 1 m/s test speed.

It has been seen that the transverse behaviour exhibited much less visco-elasticity compared to the shear behaviour. Since single values are given for the dynamic Gaussian spectrum parameters independently of the material direction, it was then decided to balance the transverse results in order not to degrade the predictability of the model in the shear behaviour. The T700GC/M21 visco-elastic transverse behaviour was then identified separately after acceptable shear parameters were obtained. The mean global error for all the transverse and shear tests was about 3.25%). A global optimisation attempt has also been done, which effectively led to a poorer global predictability of the model in the shear direction, with a mean global error of 4%.

Table 7. Final values for Berthe's bi-spectral visco-elastic model parameters values for the T700GC/M21 composite material (sequential identification of shear and transverse behaviours)

Parameter	G_{12}	n_c^{dyn}	n_0^{dyn}	n_c^{stat}	n_0^{stat}	β_{66}	γ	n	E_{22}	β_{22}
Value	11214 MPa	-11.00	5.22	3..32	2.49	1.15	1.00	2.15	12340 MPa	0.21

The E_{22} and β_{22} parameters were finally identified using the $[90]_4$ dynamic specimen geometry and the 5 mm/min, 1 m/s and creep test results. The obtained parameters are given in Table 7. with a comparison of the stress/strain curves being plotted in Fig. 10 (b) for dynamic tests and Fig. 11 (b) for creep tests.

The comparison with a purely elastic model (with an E_{22} = 10557 MPa elastic modulus value that corresponds to the apparent modulus obtained for the 1 m/s dynamic tests) is also plotted in Fig. 11(b) to demonstrate the interest of introducing the transverse visco-elastic behaviour in the model.

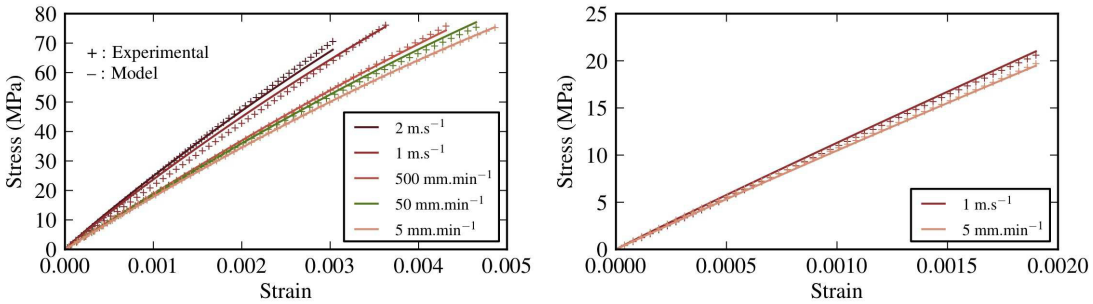

Fig. 10. Experimental versus Berthe's bi-spectral visco-elastic model results for T700GC/M21 dynamic tests (a) in shear direction; (b) in transverse direction

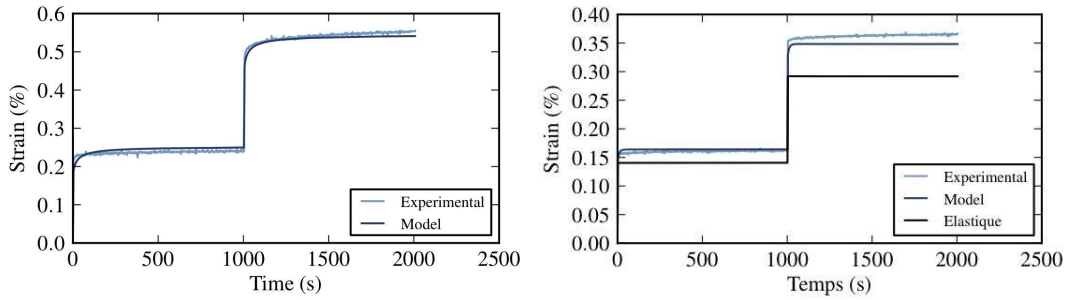

Fig. 11. Experimental versus Berthe's bi-spectral visco-elastic model results for T700GC/M21 creep tests (a) in shear direction; (b) in transverse direction

4. CONCLUSIONS AND PERSPECTIVES

The presented experimental work leads to interesting conclusions regarding strain rate dependency of the T700GC/M21 composite fibre reinforced plastic material, and possible pre-normative recommendations for the characterisation of CFRP visco-elastic models on a large range of strain rates. Concerning [±45°] specimens which are traditionally used to identify the shear behaviour of these materials (Rosen tests), a short improved geometry has been validated which give consistent quasi-static results compared to the normalized specimens. This specimen geometry has been used to perform dynamic tensile tests with strain rates varying from 10^{-3} s^{-1} to 50 s^{-1}, and creep tests which correspond to strain rates about 10^{-5} s^{-1}. An important increase (+50%) of the apparent shear modulus with the strain rate has been confirmed (from 4565 to 6621 MPa). A threshold effect regarding this strain rate dependency also appeared around 10 s^{-1}, the physical explanation of which was proposed by Berthe [7]. For the [90°] laminate, the dynamic specimen geometry has also been validated compared to quasi-static normalized test results. Dynamic and creep tests have been performed that also revealed a visco-elastic transverse behaviour, but of less amplitude than in shear.

The experimental work led to draw general conclusions and pre-normative recommendations concerning the dynamic testing of composite CFRP materials, and more specifically the formulae to be used to calculate the elastic apparent modulus from tests results obtained at different test speeds. First, for Rosen like tests that rely on [±45°] specimens, it is necessary to take care that the width of the dynamic specimens is less than half their free length (between tabs and/or grips) to avoid inhomogeneous strain distribution along the specimen mid-section (where the strain gauges are traditionally set up) that are prevented when normalized quasi-static specimens are used. A reduction in the plies number (still more than 3 plies) of the specimens was necessary to design them down to the dynamic testing machines load capabilities: this thickness reduction did not notably influence the laminate tensile visco-elastic behaviour. Note that inversely the change of specimen dimensions greatly influenced the damage onset and development in the specimens, with a more diverging non linear behaviour compared to the normalized quasi-static specimens when the strain and stress levels increase and the macroscopic damage appears. Concerning the apparent elastic modulus calculation, a direct application of the normative rules and formulae does not seem appropriate: for the [±45°] specimens, the calculation of a secant modulus on a fixed strain interval (ε =0.05% and ε =0.25% for AITM 1-0002:1998) when large visco-elastic behaviour effects are proven turned to be inaccurate since macroscopic damage might have developed in some of the specimens at highest speed tests. Last, for the [90°] specimens and the identification of the

transverse elastic modulus, the use of the ultimate stress to define the stress interval which is used to calculate the secant modulus is clearly misleading since the ultimate stress value is dramatically dispersive, especially when dynamic tests are done.

Concerning modeling aspects, a visco-elastic spectral model has been extended by Berthe to describe small strain but high strain rate CFRP behaviours. In order this model to still be used at much lower strain rates (for creep), a Gaussian bi-spectral principle has been introduced which was physically justified in Berthe's thesis because of the existence of a T_β transition temperature of the M21 resin, and the well known time-temperature equivalence for polymers. Berthe's model has been used to model the T700GC/M21 shear and transverse visco-elastic behaviour on a large strain rate range from creep (10^{-5} s^{-1}) to dynamic (50 s^{-1}) loadings. The identified set of parameters and model finally gave very good results, with a global mean error compared to the tests results that was less than 3.25%. This model is being improved by the introduction of a temperature dependency (Arrhenius law) together with the strain rate dependency: for that purpose the analysis of mechanical tests at low temperature and DMA tests are in progress that would be soon submitted for publication. The next step will concern the study of visco-damage in composite CFRP materials, meaning the strain rate and temperature influence on the onset and development of microscopic and macroscopic damage in M21 resin carbon reinforced fiber materials.

Acknowledgements

The present research work has been funded by the French Ministry of Defense and DGA (French Armament Procurement Directorate) Services. The authors are also grateful to the European Union and the French Region Nord-Pas-de-Calais for the financial support for the ONERA/DADS dynamic test facilities.

References

[1] Berthe J, Brieu M, Deletombe E, Portemont G, Lecomte-Grosbras P, Deudon A. *Consistent identification of CFRP viscoelastic models from creep to dynamic loadings*. In Strain, 49, 2013, p. 257–266.

[2] Berthe J, Brieu M, Deletombe E. *Improved viscoelastic model for laminate composite under static and dynamic loadings*. In Journal of Composite Materials, 47(14), 2013, p. 1717-1727.

[3] EN 2597 (1998). *Carbon fibre reinforced plastics. Unidirectional laminates. Tensile test perpendicular to the fibre direction*. European Committee for Standardization, Brussels, Belgium.

[4] ISO 527-5 :1997. *Plastics - Determination of tensile properties - Part 5 : Test conditions for unidirectional fibre-reinforced plastic composites*. International Standard Organisation.

[5] AITM 1–0002 (1998). *Airbus Industrie Test Method. Fibre Reinforced Plastics, Determination of in-plane shear properties*. Airbus Industrie, Blagnac, France.

[6] Rosen, B. W. *A simple procedure for experimental determination of the longitudinal shear modulus of unidirectional composites.* In Journal of Composite Materials, 6, 1972, p. 552–554.

[7] Berthe J. *Comportement thermo-visco-élastique des composites CMO - De la statique à la dynamique grande vitesse*. PhD Thesis, 2013, Ecole Centrale de Lille.

[8] Huchette C. *Sur la complémentarité des approches expérimentales et numériques pour la modélisation des mécanismes d'endommagement des composites stratifiés.* PhD Thesis, 2005, Université de Paris VI.

[9] Schieffer A. *Modélisation multiéchelle du comportement mécanique des composites à matrice organique et effets du vieillissement thermique*. PhD thesis, 2003, Université de Technologie de Troyes.

[10] Lecomte-Grosbras P, Paluch B, Brieu M, De Saxce G, Sabatier L. *Interlaminar shear strain measurement on angle-ply laminate free edge using digital image correlation.* In Composites Part A, 40(12), 2009, p. 1911–1920.

[11] Maire J-F. *Etudes théorique et expérimentale du comportement de matériaux composites en contraintes planes*. PhD thesis, 1992, Université de Franche-Comté.

[12] Laurin F, Carrère N, Maire J.-F. *A multiscale progressive failure approach for composite laminates based on thermodynamical viscoelastic and damage models.* In Composites Part A, 38, 2007, p. 198–209.

[13] Carrère N, Laurin F, Maire J-F. *Micromechanical based hybrid damage failure approach for strength predictions of composite structures.* Journal of Composite Materials, 46(19-20), 2012, p. 2389-2415.

[14] Maire J-F, Chaboche J-L. *A new formulation of continuum damage mechanics (CDM) for composite materials*. Aerospace Science and Technology, 1(4), 1997, p. 247–257.